ACS Sustainable Chemistry & Engineering

pubs.acs.org/journal/ascecg

Research Article

Guanidyl-Functionalized Magnetic Bimetallic MOF Nanocomposites Developed for Selective Enrichment of Phosphopeptides

Jia-yuan Li, Sen Zhang, Wei Gao, Yu Hua, and Hong-zhen Lian*

Cite This: *ACS Sustainable Chem. Eng.* 2020, 8, 16422−16429

Read Online

ACCESS | Metrics & More | Article Recommendations | Supporting Information

ABSTRACT: In this work, guanidine group-modified magnetic hafnium and titanium bimetallic metal−organic framework (MOF) nanocomposites denoted as Fe_3O_4@Hf/Ti-MOF-Gua were developed by a solvothermal method and post-synthetic route. Through combining metal affinity chromatography with hydrophilic interaction, the as-prepared nanomaterial was used for identifying phosphopeptides from tryptic digests of α-/β-casein by matrix-assisted laser desorption ionization-time of flight mass spectrometry and showed high sensitivity (20 fmol), high selectivity for phosphopeptides from α-/β-casein tryptic digests/phosphoprotein α-casein/BSA (1:1:2000:2000), and great reusability of three circles for capturing phosphopeptides. Because of excellent enrichment performance with a high recovery of 85.4%, this affinity probe was subsequently applied to real samples, and 27 and 15 phosphopeptides were identified from nonfat milk and human saliva, respectively. The above remarkable advantages benefitted from the strong affinity of abundant Hf^{4+}/Ti^{4+} on the large surface of the MOF shell with the improved hydrophilicity from a large number of guanidyl groups. Consequently, the novel Fe_3O_4@Hf/Ti-MOF-Gua nanocomposites not only efficiently captured phosphopeptides but also removed macromolecular proteins, indicating their great potential for the application in identification and further analysis of low-abundance phosphopeptides from complex biological samples.

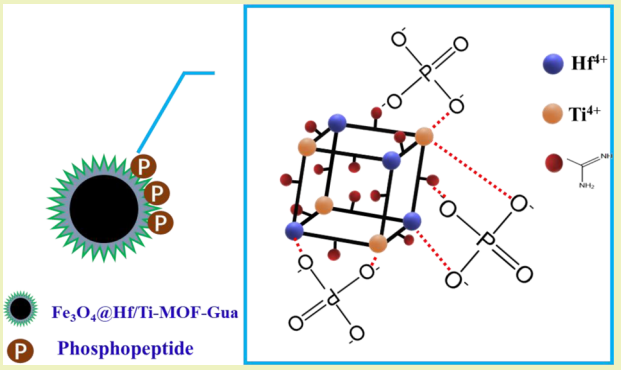

KEYWORDS: *Fe_3O_4@Hf/Ti-MOF-Gua, phosphopeptide enrichment, hydrophilicity, metal affinity chromatography, MALDI-TOF MS*

INTRODUCTION

Protein phosphorylation, which is one of the most common post-translational protein modifications, is essential in multiple biological procedures, such as enzymatic activity, immune response, and signal transduction.[1−3] Currently, one of the primary techniques to characterize phosphorylation of proteins is the bottom-up strategy. Matrix-assisted laser desorption ionization-time of flight mass spectrometry (MALDI-TOF MS) has been widely used in biological analysis for its fast speed, high throughput, resolution, and efficiency.[4] Nevertheless, because of the low levels of phosphopeptides and strong signal suppression from the abundance of non-phosphopeptides, it remains a great challenge to directly analyze phosphopeptides by MALDI-TOF MS.[5] Thus, sample pretreatment including effective and selective enrichment process of phosphopeptides is necessary prior to MS analysis.

To date, varieties of functional affinity materials have been developed for the enrichment of phosphospeptides from nonphosphopeptides,[6] including immobilized metal affinity materials,[7,8] metal oxide materials,[9] graphene-based materials,[10] and metal−organic framework (MOF)-based materials.[11] Among these above materials, MOFs, with extremely high porosity, enormous internal surface areas, chemical tenability, and easy for functional modification, are known as porous crystalline materials by linking organic ligands with metal centers to form infinite arrays through dative bonds.[12] In combination with the abundant metal sites toward phosphospeptides and the distinct porosity excluding large-sized substances in the meantime, MOFs have been successfully applied as affinity probes toward phosphopeptides.[13,14] To improve the enrichment efficiency of MOFs for detecting phosphopeptides, phosphate-philic and/or hydrophilic groups have been modified on the surface of MOFs via post-synthetic modification.[15,16] Recently, Gu's group prepared two-dimensional MOF nanosheets for selective capture of monophosphopeptides, followed by MALDI-TOF MS analysis.[17] However, the separation process of MOF affinity materials toward phosphopeptides through centrifugation is slightly tedious. In addition, MOFs could be incorporated into

Received: June 6, 2020
Revised: October 1, 2020
Published: October 29, 2020

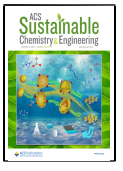

monolithic capillary to distinguish phosphopeptides by MALDI-TOF MS.[18] Nevertheless, the monolithic capillaries for phosphopeptide enrichment are seldom reported probably owing to the difficulty in preparation, instability, and low capacity.

Because of rapid magnetic separation and plenty of metal-containing units, magnetic MOFs as promising materials have attracted increasing attention in phosphopeptide enrichment.[19−23] Certain functionalized magnetic MOFs as multifunctional probes exhibited excellent performance in both phosphopeptide and glycopeptide enrichment.[24−28] Very interestingly, bimetallic MOFs possessed unique property resulting from the co-consistence of multiple metals compared with single metal MOFs, being devoted to distinguish phosphopeptides from complex biological samples.[29−31] However, the elements chosen for bimetallic MOFs to facilitate phosphopeptide enrichment were limited to zirconium-titanium. As a group of element with a chemical property similar to Zr and Ti, high-valence metal Hf could also be used as a central ion to obtain MOFs toward phosphopeptides.[17] Herein, for the first time, amino-functionalized hafnium-titanium bimetallic MOFs (Hf/Ti-MOF-NH_2) designed for post modification were decorated on the surface of Fe_3O_4 nanoparticles. Based on the abundant amino groups in amino-functionalized magnetic bimetallic MOFs (Fe_3O_4@Hf/Ti-MOF-NH_2), guanidyl-functionalized magnetic bimetallic MOF nanocomposites (denoted as Fe_3O_4@Hf/Ti-MOF-Gua) were prepared via a post-synthetic route and subsequently utilized as an affinity probe for highly selective separation of phosphopeptides, exhibiting great hydrophilicity, high surface area, size exclusion effect, and strong magnetic responsiveness and anticipating an excellent performance in the capture of phosphopeptide with ultrahigh sensitivity and selectivity.

EXPERIMENTAL SECTION

Synthesis of Fe_3O_4@Hf/Ti-MOF-Gua. The workflow for the preparation of Fe_3O_4@Hf/Ti-MOF-Gua is demonstrated in Scheme 1A. First, Fe_3O_4 nanoparticles were fabricated via a solvothermal method.[32,33] Then, Fe_3O_4 (100 mg) was mixed with $HfCl_4$ (160 mg), titanium(IV) *n*-butoxide (0.13 mL), 2-aminoterephthalic acid (272 mg), CH_3OH (4 mL), and DMF (36 mL), followed by sonication and stirring at room temperature for 30 min. After the mixture was transferred to a 50 mL Teflon liner and heated at 125 °C for 24 h, amino-functionalized magnetic bimetallic MOFs (Fe_3O_4@Hf/Ti-MOF-NH_2) were collected by an external magnetic field and washed with DMF and water, respectively. Guanidyl-functionalized magnetic bimetallic MOF nanocomposites (Fe_3O_4@Hf/Ti-MOF-Gua) were synthesized as follows. Fe_3O_4@Hf/Ti-MOF-NH_2 nanoparticles (50 mg) were dispersed into 50 mL of *O*-methylisourea hemisulfate solution (3.081 g, pH 11) and heated at 60 °C for 24 h. Ultimately, Fe_3O_4@Hf/Ti-MOF-Gua nanocomposites were obtained by magnetic separation. For comparison, Fe_3O_4@Hf-MOF-Gua and Fe_3O_4@Ti-MOF-Gua nanocomposites were, respectively, synthesized according to the same procedure of Fe_3O_4@Hf/Ti-MOF-Gua except that only one metal source was used, and Fe_3O_4@Hf/Ti-MOF nanocomposites were prepared similar to Fe_3O_4@Hf/Ti-MOF-NH_2 using terephthalic acid instead of 2-aminoterephthalic acid, which are detailed in the Supporting Information.

Sample Preparation. α-/β-Casein and nonfat milk trypsin digests were prepared based on our previous work[34] with minor modifications. Detailed procedures are shown in the Supporting Information. The above biological samples were stored at −80 °C for further use.

Enrichment of Phosphopeptides with Fe_3O_4@Hf/Ti-MOF-Gua Nanocomposites from Different Samples. The workflow for enriching phosphopeptides is shown in Scheme 1B according to our previous work[35,36] with minor modifications. Briefly, 5.0 μL of Fe_3O_4@Hf/Ti-MOF-Gua (20 mg mL^{-1}) was added at room temperature into 100 μL of peptide mixture. The peptide mixture was originated from a mixture of tryptic digests of α-/β-casein (2.5 μL) or tryptic digests of nonfat milk (1.0 μL), or human saliva (1.0 μL), which was diluted to 1 mL with 50% ACN—0.5% TFA solution, respectively. Accompanied by Fe_3O_4@Hf/Ti-MOF-Gua probes, the mixture was then vortexed at room temperature for 15 min, after which the phosphopeptide-loaded probes were gathered with the help of exterior magnetic field and rinsed using 50% ACN—0.1% TFA solution (100 μL) three times. Subsequently, 5 μL of $NH_3{\cdot}H_2O$ (10%, w/w) was used to elute the trapped phosphopeptides by sonication for 10 min. Finally, after rapid magnetic separation, these supernatants were isolated for MALDI-TOF MS analysis. MS analysis and database searching were performed according to our previous reports[33,35] with minor modifications (see the Supporting Information). Fe_3O_4, Fe_3O_4@Hf/Ti-MOF, and Fe_3O_4@Hf/Ti-MOF-NH_2, as well as Fe_3O_4@Hf-MOF-Gua and Fe_3O_4@Ti-MOF-Gua, were also used to capture phosphopeptides as comparison.

Enrichment Recovery of Phosphopeptides with Fe_3O_4@Hf/Ti-MOF-Gua Nanocomposites. The operation of stable isotope dimethyl labeling was processed as previous work[36,37] with minor modifications. Briefly, the solution of LRRApSLGGK (a standard phosphopeptide) was divided into two aliquots and then labeled with CH_2O or CD_2O, resulting in a mass increase of 28 or 32 Da, respectively. After being captured by Fe_3O_4@Hf/Ti-MOF-Gua following the enrichment procedure mentioned above, the acquired eluate of the heavy labeled phosphopeptide was mixed with the equal volume of the light-labeled phosphopeptide solution for MS analysis.

Scheme 1. Synthesis Strategy of Fe_3O_4@Hf/Ti-MOF-Gua Nanocomposites (A) and Enrichment of Phosphopeptides from Biological Samples Using Fe_3O_4@Hf/Ti-MOF-Gua as the Affinity Probe (B)

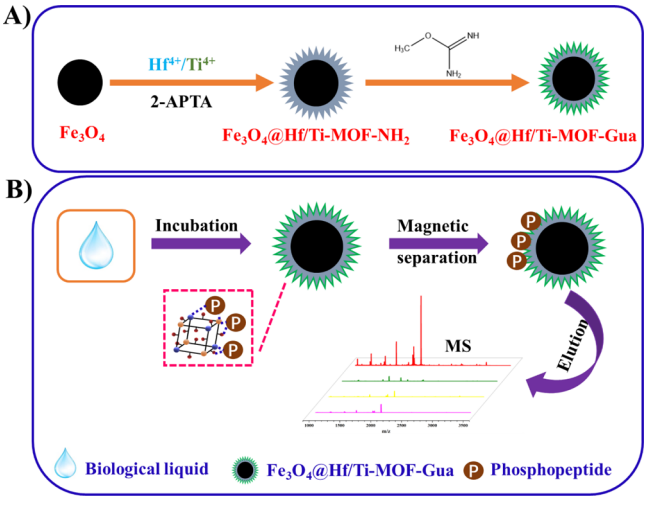

RESULTS AND DISCUSSION

Characterization of Fe_3O_4@Hf/Ti-MOF-Gua. The morphology and microstructure of all three nanomaterials were characterized by transmission electron microscopy (TEM) and scanning electron microscopy (SEM) images. Fe_3O_4 nanoparticles had a uniform spherical morphology and good monodispersity with a mean grain size of 200 nm (Figure 1A), while Fe_3O_4@Hf/Ti-MOF-NH_2 exhibited the thin and irregular MOF shells around the surface of Fe_3O_4 nanoparticles (Figure 1B). After modification with guanidine functional groups, the surface of as-prepared Fe_3O_4@Hf/Ti-MOFs-Gua

https://dx.doi.org/10.1021/acssuschemeng.0c04118
ACS Sustainable Chem. Eng. 2020, 8, 16422−16429

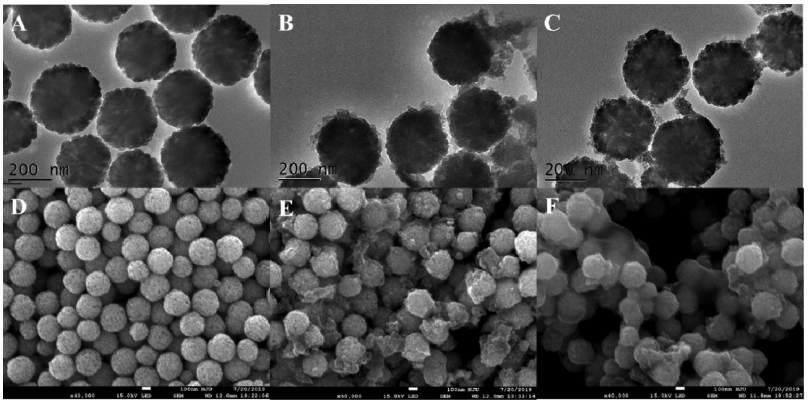

Figure 1. TEM images of Fe_3O_4 (A), Fe_3O_4@Hf/Ti-MOF-NH_2 (B), and Fe_3O_4@Hf/Ti-MOF-Gua (C); SEM images of Fe_3O_4 (D), Fe_3O_4@Hf/Ti-MOF-NH_2 (E), and Fe_3O_4@Hf/Ti-MOF-Gua (F).

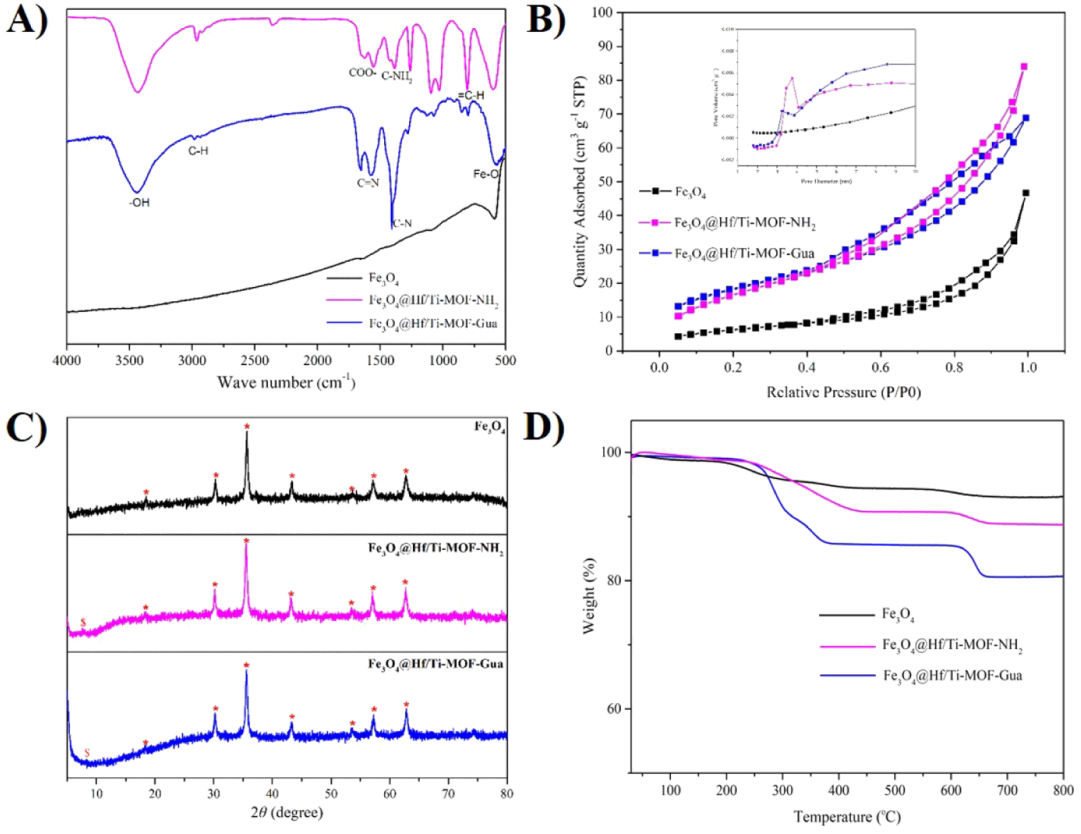

Figure 2. FT-IR spectra (A), N_2 adsorption−absorption isotherms, with pore size distribution curves inset (B), XRD patterns (C), and TGA curves (D) of Fe_3O_4, Fe_3O_4@Hf/Ti-MOF-NH_2, and Fe_3O_4@Hf/Ti-MOF-Gua.

nanocomposites was rather rougher (Figure 1C), which was distinct from that of Fe_3O_4@Hf/Ti-MOF-NH_2. In addition, the surface features of Fe_3O_4, Fe_3O_4@Hf/Ti-MOF-NH_2, and Fe_3O_4@Hf/Ti-MOFs-Gua characterized by SEM were in accordance with the TEM results by analysis, respectively (Figure 1D−F). The energy-dispersive spectroscopy (EDS) spectra shown in Figure S1A−C identified the elemental composition of the above three materials. Both Hf and Ti elements emerged in Fe_3O_4@Hf/Ti-MOF-NH_2, illustrating the successful coating of bimetallic MOF layers on the surface of Fe_3O_4 nanoparticles. The contents of Hf and Ti were 0.47 and 0.35%, respectively, indicating that more Hf entered the nanocomposites than Ti (1.34:1). Then, after modification with guanidine functional groups, the content of N increased from 0.11 to 0.28 wt %, with the Hf/Ti ratio almost kept unchanged at 1.28:1 and mainly owing to introduction of additional *N* element from guanidine functional groups. Moreover, EDS-mapping images of O, Fe, Hf, Ti, and N elements from Fe_3O_4@Hf/Ti-MOF-Gua (Figure S1D−H) displayed the homogeneous distribution of the above elements in the nanocomposites. In addition, more Hf compared with Ti were also observed from EDS-mapping images of Fe_3O_4@Hf/Ti-MOF-Gua (Figure S1F,G). As shown in Figure S1H,I, more N element distributed in Fe_3O_4@Hf/Ti-MOF-Gua was further testified than that in Fe_3O_4@Hf/Ti-MOF-NH_2.

In order to confirm the modification with the guanidyl-functionalized MOF layers on the surface of Fe_3O_4 nanoparticles, some other corresponding characterization experi-

https://dx.doi.org/10.1021/acssuschemeng.0c04118
ACS Sustainable Chem. Eng. 2020, 8, 16422−16429

ments were carried out. As seen in Figure 2A, there were several new peaks in the Fourier-transform infrared (FT-IR) spectrum of Fe_3O_4@Hf/Ti-MOF-NH_2 compared with that of Fe_3O_4 (570 cm^{-1}, $\nu_{Fe-O-Fe}$). The peak of 3425 cm^{-1} was ascribed to the stretching vibration of N−H, and the peaks of 2975 and 2856 cm^{-1} were attributed to asymmetric and symmetric C−H stretching vibrations, respectively. The peaks of 1635 and 1566 cm^{-1} belonged to the stretching vibration of aromatic rings, and the peaks of 1382 and 1101 cm^{-1} corresponded closely to the C−N stretching vibration and C−NH_2 bending vibration, respectively. Besides, the FT-IR spectrum of Fe_3O_4@Hf/Ti-MOF-Gua has changed slightly relative to Fe_3O_4@Hf/Ti-MOF-NH_2, with the peak of 1382 cm^{-1} enhanced because of immobilization of guanidine functional groups. Moreover, to evaluate the specific surface area and porous structure of the prepared nanocomposites, N_2 adsorption−desorption isotherms were drawn (Figure 2B). The Brunauer−Emmett−Teller surface areas of Fe_3O_4, Fe_3O_4@Hf/Ti-MOF-NH_2, and Fe_3O_4@ Hf/Ti-MOF-Gua were calculated to be 22.71, 65.23, and 64.25 $m^2 \cdot g^{-1}$, respectively. At the same time, it was found that a new pore diameter of 3.5 nm emerged after coating amino-functionalized MOF layers to Fe_3O_4 nanoparticles, and then the pore diameter decreased to 3.2 nm after further modification with guanidine functional groups on the MOF layers. Obviously, after being coated with the MOF shell, the surface area of resulting nanomaterials increased a lot in comparison with that of original Fe_3O_4 cores. However, the introduction of abundant guanidyl groups that occupied a certain space in the structure of the MOF shell led to a slight decrease in surface area and pore diameter compared to amino groups. The above results suggested that the guanidine group-modified core−shell structured magnetic MOF distinguished by abundant Hf^{4+}/Ti^{4+} sites and large specific areas is a potential adsorbent for phosphopeptides excluding large molecular weight proteins. X-ray diffraction (XRD) patterns of Fe_3O_4 nanoparticles presented typical diffraction peaks at 18.3, 30.3, 35.2, 43.5, 53.4, 57.1, and 62.8°, which responded, respectively, to the 111, 220, 311, 400, 422, 511, and 440 faces of Fe_3O_4 (JCPD no. 19-06290). For Fe_3O_4@Hf/Ti-MOF-NH_2 and Fe_3O_4@ Hf/Ti-MOF-Gua, a new diffraction peak at 7.8° could be indexed to the crystalline structure of Hf/Ti-based MOF, relating to the MOF shells formed on the surface of Fe_3O_4 nanoparticles (Figure 2C). Thermogravimetric (TGA) analysis was performed in the range of 25−800 °C to check chemical components (Figure 2D). The weight loss of Fe_3O_4 during the whole heating process was slight,[36] whereas Fe_3O_4@Hf/Ti-MOF-NH_2 and Fe_3O_4@Hf/Ti-MOF-Gua underwent two steps of significant thermal decomposition. The mass loss of Fe_3O_4@Hf/Ti-MOF-NH_2 nanocomposites was calculated to be 11.7 wt %, while that of Fe_3O_4@Hf/Ti-MOF-Gua nanocomposites increased to as high as 19.8 wt %, indicating the introduction of abundant organic functional groups after immobilization with guanidyl groups.

Meanwhile, the magnetic measurement was carried out at room temperature in order to evaluate the magnetic behavior of the prepared nanocomposites. According to the magnetic hysteresis loops in Figure S2, Fe_3O_4, Fe_3O_4@Hf/Ti-MOF-NH_2, and Fe_3O_4@Hf/Ti-MOF-Gua all possessed a typical superparamagnetic property with the saturation magnetization (M_s) values of 70.0, 53.8, and 49.8 emu g^{-1}, respectively. The superparamagnetic performance suggested that Fe_3O_4@Hf/Ti-MOF-Gua nanocomposites could be isolated rapidly with a magnet. After removing the magnetic field, the affinity probes can be dispersed into solution again, which were suitable for the magnetic separation process. In addition, the TEM and SEM characterization results of Fe_3O_4@Hf/Ti-MOF, as well as Fe_3O_4@Hf-MOF-Gua and Fe_3O_4@Ti-MOF-Gua, are shown in Figures S3−S5, indicating the successful synthesis of three magnetic MOF materials for comparison.

Enrichment Performance of Fe_3O_4@Hf/Ti-MOF-Gua Nanocomposites for Phosphopeptides. In order to evaluate the universality of Fe_3O_4@Hf/Ti-MOF-Gua nanocomposites in enrichment of phosphopeptides, 10 pmol of α-/β-casein tryptic digests (molar ratio 1:1) was employed as model samples. For comparison, Fe_3O_4, Fe_3O_4@Hf/Ti-MOF, and Fe_3O_4@Hf/Ti-MOF-NH_2 were also applied as affinity probes toward phosphopeptides. Considering that the acidity usually plays a critical role in phosphopeptide enrichment, 50% ACN with different TFA concentrations (0.01−1.0%) was used as a loading buffer (Figures S6−S8). Under individually optimized acidity condition for each material, the phosphopeptide enrichment experiment was carried out. Before enrichment, only four phosphopeptides (m/z 1952, 2061, 2555, 3122) with a weak signal intensity and low signal-to-noise ratio (S/N) of MS were detected, whereas several nonphosphopeptides were predominant (Figure 3A). After treatment with

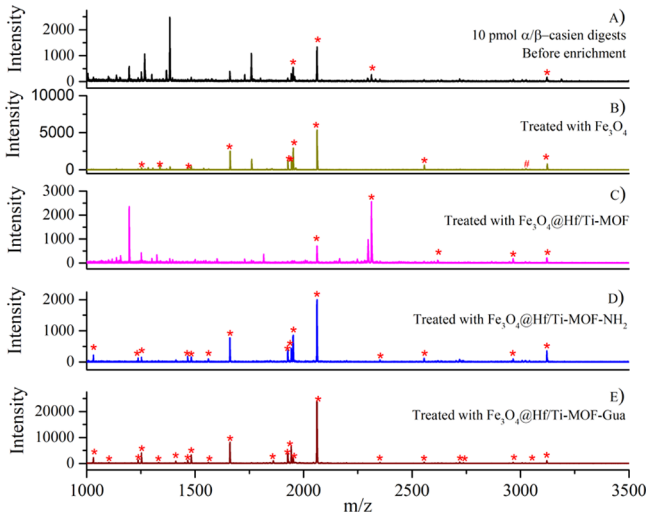

Figure 3. MS of α-/β-casein tryptic digests (v/v = 1:1) before (A) and after enrichment by different materials: Fe_3O_4 (B), Fe_3O_4@Hf/Ti-MOF (C), Fe_3O_4@Hf/Ti-MOF-NH_2 (D), and Fe_3O_4@Hf/Ti-MOF-Gua (E). Optimal TFA concentration: 1.0% for Fe_3O_4, 1.0% for Fe_3O_4@Hf/Ti-MOF, 0.5% for Fe_3O_4@Hf/Ti-MOF-NH_2, and 0.5% for Fe_3O_4@Hf/Ti-MOF-Gua. "*" denotes phosphopeptides, "#" denotes dephosphorylated residues from phosphopeptides.

Fe_3O_4, 10 phosphopeptides exhibited relatively low intensity with bits of nonphosphopeptides in the MS spectrum (Figure 3B). Although pretreated with Fe_3O_4@Hf/Ti-MOF, nonphosphopeptide could not be completely removed (Figure 3C) because of the lack of selectivity to phosphopeptides. Fe_3O_4@ Hf/Ti-MOF-NH_2 can selectively capture phosphopeptides excluding nonphosphopeptides, implying that hydrophilic amino groups could improve the probe ability to enrich hydrophilic phosphopeptides (Figure 3D). Moreover, after treatment with Fe_3O_4@Hf/Ti-MOF-Gua, the most number of phosphopeptides with the strongest signal intensity dominated the MS spectrum with disappearance of nonphosphopeptides

https://dx.doi.org/10.1021/acssuschemeng.0c04118
ACS Sustainable Chem. Eng. 2020, 8, 16422−16429

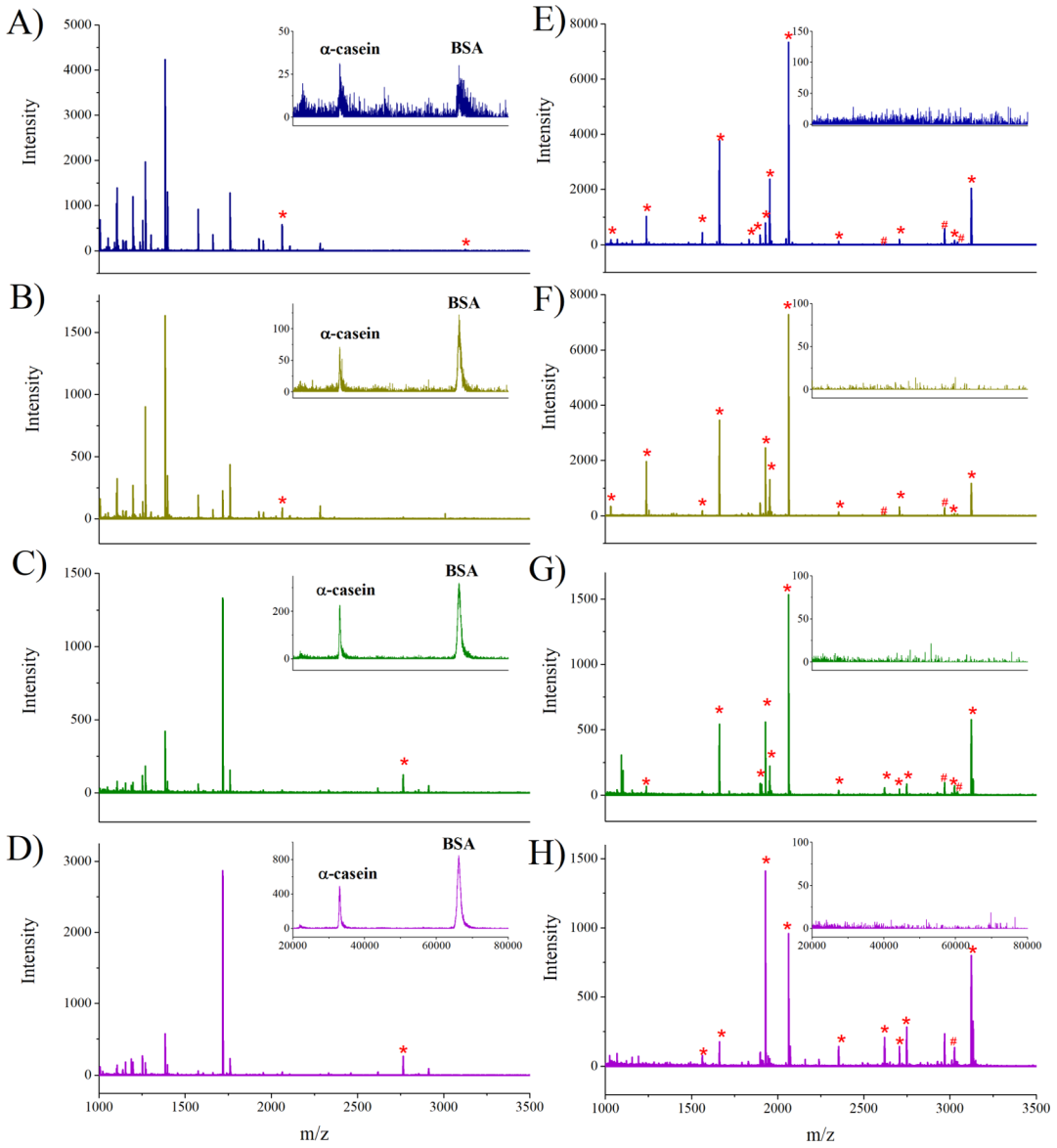

Figure 4. MS of α-/β-casein tryptic digests and standard protein α-casein and BSA at different mass ratios of 1:1:10:10, 1:1:100:100, 1:1:1000:1000, and 1:1:2000:2000 before (A–D, respectively) and after enrichment by Fe_3O_4@Hf/Ti-MOF-Gua affinity probe (E–H, respectively). "*" denotes phosphopeptides, "#" denotes dephosphorylated residues from phosphopeptides.

(Figure 3E). In addition, magnetic single-metal MOFs modified by guanine groups, Fe_3O_4@Hf-MOF-Gua and Fe_3O_4@Ti-MOF-Gua, exhibited inferior performance in phosphopeptide enrichment compared with Fe_3O_4@Hf/Ti-MOF-Gua (Figures S9 and S10). This is probably attributed to the synergy of affinity interaction of metallic Hf^{4+}/Ti^{4+} and hydrophilic interaction of guanidine groups from the MOF shell in Fe_3O_4@Hf/Ti-MOF-Gua nanocomposites toward phosphate groups in phosphopeptides. Table S1 lists the detailed information of the identified phosphopeptides enriched from tryptic digests of α-/β-casein.

To assess the sensitivity of Fe_3O_4@Hf/Ti-MOF-Gua as well as Fe_3O_4@Hf-MOF-Gua and Fe_3O_4@Ti-MOF-Gua nanocomposites in the enrichment of phosphopeptides, the affinity probes were added to different concentrations of α-/β-casein tryptic digests for capturing phosphopeptides (Figures S11 and S12). At least one phosphopeptide can still be clearly identified even under low levels of 20, 25, and 50 fmol α-/β-casein tryptic digests, respectively, by the three above-mentioned materials, illustrating that the as-prepared Fe_3O_4@Hf/Ti-MOF-Gua has higher enrichment sensitivity toward phosphopeptides than two single-metal MOF nanocomposites, Fe_3O_4@Hf-MOF-Gua and Fe_3O_4@Ti-MOF-Gua. To test the selectivity of Fe_3O_4@Hf/Ti-MOF-Gua nanocomposites in the enrichment of phosphopeptides, different amounts of standard phosphoprotein α-casein and non-phosphoprotein BSA were added to α-/β-casein tryptic digests (Figure 4). With the increase of interfering substances α-casein and BSA added, nonphosphopeptide peaks as well as the mass signals of proteins dominated the spectrum, while phosphopeptide peaks were suppressed before enrichment. In contrast, after capture by this affinity probe, phosphopeptide peaks were detected with strong signal intensity excluding the influence of abundant nonphosphopeptides, phosphoprotein, and non-phosphoprotein. Even when α-casein and BSA were at the dosages of 2000-fold compared to that of α-/β-casein digests, phosphopeptide peaks could still be detected with a clear background, showing the superselectivity of Fe_3O_4@Hf/Ti-MOF-Gua for the

https://dx.doi.org/10.1021/acssuschemeng.0c04118
ACS Sustainable Chem. Eng. 2020, 8, 16422–16429

enrichment of phosphopeptides. This is mainly ascribed to the mesoporous structures in the MOF shell from Fe_3O_4@Hf/Ti-MOF-Gua, possessing size exclusion selectivity toward high-molecular-weight proteins from phosphopeptides.

In order to examine the repeatability and stability of Fe_3O_4@Hf/Ti-MOF-Gua nanocomposites in the enrichment of phosphopeptides, the affinity probes were recycled by washing with the 50% ACN−0.5% TFA solution several times. As seen in Figure S13, after being used and regenerated three times, Fe_3O_4@Hf/Ti-MOF-Gua affinity probe could still capture phosphopeptides effectively, and the peak intensity in MS spectra was not attenuated obviously. On every account, the affinity probe exhibited robust specificity as well as excellent reusability toward phosphopeptides based on the above results. To evaluate the enrichment recovery of Fe_3O_4@Hf/Ti-MOF-Gua nanocomposites toward phosphopeptides, a standard phosphopeptide (LRRApSLGGK) was utilized as a model sample. The recovery of this phosphopeptide was calculated to be as high as 85.4% (Figure S14), indicating that this affinity probe could work as an effective and satisfactory adsorbent to enrich phosphopeptides.

To investigate the capacity of Fe_3O_4@Hf/Ti-MOF-Gua nanocomposites for enriching phosphopeptides, *p*-nitrophenylphospahte (pNPP) was used as a model compound. As shown in Figure S15, the adsorption capacities of pNPP with Fe_3O_4@/Ti-MOF-Gua, Fe_3O_4@Hf-MOF-Gua, and Fe_3O_4@Ti-MOF-Gua were measured to be 138.46, 73.65, and 49.74, mg g^{-1}, respectively, revealing excellent ability of Fe_3O_4@Hf/Ti-MOF-Gua toward phosphopeptides compared with the investigated monometallic MOF nanocomposites.

Enrichment of Phosphopeptides from Real Samples by Fe_3O_4@Hf/Ti-MOF-Gua Nanocomposites. Inspired by the results of the above-mentioned experiments, further research using nonfat milk and human saliva as real samples was conducted for examining the practical application of Fe_3O_4@Hf/Ti-MOF-Gua nanocomposites toward phosphopeptides. As seen from Figure S16, there were only four phosphopeptides detected directly in nonfat milk with low MS peak intensity. On the contrary, 27 phosphopeptides with high signal intensity were easily observed after the treatment with this affinity probe, excluding the interference of nonphosphopeptides. The enrichment performance of Fe_3O_4@Hf/Ti-MOF-Gua is superior to those of Fe_3O_4, Fe_3O_4@Hf/Ti-MOF, and Fe_3O_4@Hf/Ti-MOF-NH_2 toward phosphopeptides in nonfat milk, which is similar to the result for *α*-/*β*-casein tryptic digests. Table S2 lists the detailed information of the identified phosphopeptides enriched by the Fe_3O_4@Hf/Ti-MOF-Gua probe. As is well known, there are probably potential markers including endogenous phosphopeptides in human saliva for diagnosis and therapy.[38,39] Yet, it is difficult to directly detect phosphopeptides in saliva because of the low levels combining with interferences of the complex matrix. In the present experiment, there was only one phosphopepitde peak recognized from human saliva by direct analysis of MS, which was dominated by a large number of nonphosphopeptides peaks (Figure 5A). In addition, there were large amounts of high-molecular-weight substances which probably are plentiful proteins in the human saliva sample. After treatment with Fe_3O_4@Hf/Ti-MOF-Gua nanocomposites, 15 phosphopeptides were observed in MS with a clear background (Figure 5B), and the high-molecular impurities were removed owing to the size exclusion of outermost MOF layers as well. Table S3 lists the detailed information of the phosphopeptides enriched from saliva by this affinity probe. These results confirmed the outstanding practical applicability of Fe_3O_4@Hf/Ti-MOF-Gua for phosphopeptide enrichment.

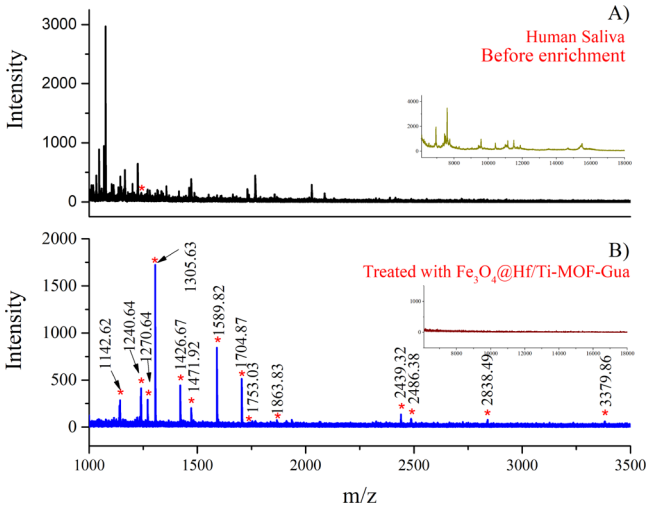

Figure 5. MS of human saliva before (A) and after enrichment by Fe_3O_4@Hf/Ti MOF-Gua affinity probe (B).

Comparison with Other MOF Affinity Probes toward Phosphopeptides. Detailed comparisons of Fe_3O_4@Hf/Ti-MOF-Gua with other MOF affinity probes for phosphopeptides are summarized in Table S4 on the aspects of material amount, separation mode, enrichment selectivity, and application. Compared with these existing materials including monometallic MOFs, it is proven that the developed Fe_3O_4@Hf/Ti-MOF-Gua nanocomposites in this work have considerable enrichment performance. Furthermore, the magnetic separation mode made the enrichment process by the probe more convenient and rapid in comparison with that by nonmagnetic nanomaterials.

CONCLUSIONS

In summary, bimetallic MOFs (Hf/Ti-MOF-NH_2) were designed and assembled on the surface of Fe_3O_4 nanoparticles by a facile solvothermal method, and guanidyl groups were then modified via a post-synthetic route to obtain Fe_3O_4@Hf/Ti-MOF-Gua nanocomposites. After sufficient property characterization, Fe_3O_4@Hf/Ti-MOF-Gua was applied in the highly selective enrichment of phosphopeptides, excluding high-molecular-weight proteins. Owing to coexistence of abundant Hf^{4+}/Ti^{4+}, high surface area of mesoporous structures in the MOF shell, excellent hydrophilicity from a large amount of guanidyl groups, and strong magnetic responsiveness of Fe_3O_4 cores, this affinity probe possessed a great performance in phosphopeptide enrichment with ultrahigh sensitivity and selectivity, excellent reusability, and high enrichment recovery. Therefore, the findings of the first attempt for Fe_3O_4@Hf/Ti-MOF-Gua are interesting and promising in the separation of low-abundance phosphopeptides from real-world biological samples containing very high levels of proteins including phosphopeptides and nonphosphopeptides.

ASSOCIATED CONTENT

Supporting Information

The Supporting Information is available free of charge at https://pubs.acs.org/doi/10.1021/acssuschemeng.0c04118.

https://dx.doi.org/10.1021/acssuschemeng.0c04118
ACS Sustainable Chem. Eng. 2020, 8, 16422−16429

EDS spectra of Fe_3O_4, Fe_3O_4@Hf/Ti-MOF-NH_2, and Fe_3O_4@Hf/Ti-MOF-Gua; hysteresis loops of the three above-mentioned materials; characterization of Fe_3O_4@Hf/Ti-MOF, Fe_3O_4@Hf-MOF-Gua, and Fe_3O_4@Ti-MOF-Gua; sample preparation; performance of Fe_3O_4@Hf/Ti-MOF-Gua and other affinity probes in the enrichment of phosphopeptides; amino acid sequence of phosphopeptides identified from α-/β-casein tryptic digests, nonfat milk, as well as human saliva after enrichment by Fe_3O_4@Hf/Ti-MOF-Gua nanocomposites; and detailed comparisons of the Fe_3O_4@Hf/Ti-MOF-Gua affinity probes with existing MOF affinity probes (PDF).

AUTHOR INFORMATION

Corresponding Author

Hong-zhen Lian − *State Key Laboratory of Analytical Chemistry for Life Science, School of Chemistry & Chemical Engineering and Center of Materials Analysis, Nanjing University, Nanjing 210023, China;* orcid.org/0000-0003-1942-9248; Phone: +86-25-83686075; Email: hzlian@nju.edu.cn; Fax: +86-25-83325180

Authors

Jia-yuan Li − *State Key Laboratory of Analytical Chemistry for Life Science, School of Chemistry & Chemical Engineering and Center of Materials Analysis, Nanjing University, Nanjing 210023, China*

Sen Zhang − *State Key Laboratory of Analytical Chemistry for Life Science, School of Chemistry & Chemical Engineering and Center of Materials Analysis, Nanjing University, Nanjing 210023, China*

Wei Gao − *State Key Laboratory of Analytical Chemistry for Life Science, School of Chemistry & Chemical Engineering and Center of Materials Analysis, Nanjing University, Nanjing 210023, China*

Yu Hua − *State Key Laboratory of Analytical Chemistry for Life Science, School of Chemistry & Chemical Engineering and Center of Materials Analysis, Nanjing University, Nanjing 210023, China*

Complete contact information is available at: https://pubs.acs.org/10.1021/acssuschemeng.0c04118

Notes

The authors declare no competing financial interest.

ACKNOWLEDGMENTS

This work was supported by the National Natural Science Foundation of China (grant nos. 21874065, 91643105, 21577057), as well as the Natural Science Foundation of Jiangsu Province (grant no. BK20171335).

REFERENCES

(1) Olsen, J. V.; Blagoev, B.; Gnad, F.; Macek, B.; Kumar, C.; Mortensen, P.; Mann, M. Global, in vivo, and site-specific phosphorylation dynamics in signaling networks. *Cell* **2006**, *127*, 635−648.

(2) Huttlin, E. L.; Jedrychowski, M. P.; Elias, J. E.; Goswami, T.; Rad, R.; Beausoleil, S. A.; Villén, J.; Haas, W.; Sowa, M. E.; Gygi, S. P. A tissue-specific atlas of mouse protein phosphorylation and expression. *Cell* **2010**, *143*, 1174−1189.

(3) Wiseman, R. L.; Kelly, J. W. Phosphatase inhibition delays translational recovery. *Science* **2011**, *332*, 44−45.

(4) Domon, B.; Aebersold, R. Review - mass spectrometry and protein analysis. *Science* **2006**, *312*, 212−217.

(5) Boersema, P. J.; Mohammed, S.; Heck, A. J. R. Phosphopeptide fragmentation and analysis by mass spectrometry. *J. Mass Spectrom.* **2009**, *44*, 861−878.

(6) Li, X.-S.; Yuan, B.-F.; Feng, Y.-Q. Recent advances in phosphopeptide enrichment: strategies and techniques. *TrAC, Trends Anal. Chem.* **2016**, *78*, 70−83.

(7) Sun, X.; Liu, X.; Feng, J.; Li, Y.; Deng, C.; Duan, G. Hydrophilic Nb^{5+}-immobilized magnetic core-shell microsphere - a novel immobilized metal ion affinity chromatography material for highly selective enrichment of phosphopeptides. *Anal. Chim. Acta* **2015**, *880*, 67−76.

(8) Zhao, M.; Deng, C.; Zhang, X. The design and synthesis of a hydrophilic core-shell-shell structured magnetic metal-organic framework as a novel immobilized metal ion affinity platform for phosphoproteome research. *Chem. Commun.* **2014**, *50*, 6228−6231.

(9) Cheng, G.; Zhang, J.-L.; Liu, Y.-L.; Sun, D.-H.; Ni, J.-Z. Synthesis of novel Fe_3O_4@SiO_2@CeO_2 microspheres with mesoporous shell for phosphopeptide capturing and labeling. *Chem. Commun.* **2011**, *47*, 5732−5734.

(10) Xu, L.-N.; Li, L.-P.; Jin, L.; Bai, Y.; Liu, H.-W. Guanidyl-functionalized graphene as a bifunctional adsorbent for selective enrichment of phosphopeptides. *Chem. Commun.* **2014**, *50*, 10963−10966.

(11) Yang, S.-S.; Shi, M.-Y.; Tao, Z.-R.; Wang, C.; Gu, Z.-Y. Recent applications of metal-organic frameworks in matrix-assisted laser desorption/ionization mass spectrometry. *Anal. Bioanal. Chem.* **2019**, *411*, 4509−4522.

(12) Furukawa, H.; Cordova, K. E.; O'Keeffe, M.; Yaghi, O. M. The chemistry and applications of metal-organic frameworks. *Science* **2013**, *341*, 1230444.

(13) Peng, J.; Wu, R. A. Metal-organic frameworks in proteomics/peptidomics - a review. *Anal. Chim. Acta* **2018**, *1027*, 9−21.

(14) Peng, J.; Zhang, H.; Li, X.; Liu, S.; Zhao, X.; Wu, J.; Kang, X.; Qin, H.; Pan, Z.; Wu, R. A. Dual-metal centered zirconium-organic framework: a metal-affinity probe for highly specific interaction with phosphopeptides. *ACS Appl. Mater. Interfaces* **2016**, *8*, 35012−35020.

(15) Yang, X.; Xia, Y. Urea-modified metal-organic framework of type MIL-101(Cr) for the preconcentration of phosphorylated peptides. *Microchim. Acta* **2016**, *183*, 2235−2240.

(16) Peng, J.; Niu, H.; Zhang, H.; Yao, Y.; Zhao, X.; Zhou, X.; Wan, L.; Kang, X.; Wu, R. A. Highly specific enrichment of multi-phosphopeptides by the diphosphorylated fructose-modified dual-metal-centered zirconium-organic framework. *ACS Appl. Mater. Interfaces* **2018**, *10*, 32613−32621.

(17) Yang, S.-S.; Chang, Y.-J.; Zhang, H.; Yu, X.; Shang, W.; Chen, G.-Q.; Chen, D. D. Y.; Gu, Z.-Y. Enrichment of phosphorylated peptides with metal-organic framework nanosheets for serum profiling of diabetes and phosphoproteomics analysis. *Anal. Chem.* **2018**, *90*, 13796−13805.

(18) Li, D.; Bie, Z. Metal-organic framework incorporated monolithic capillary for selective enrichment of phosphopeptides. *RSC Adv.* **2017**, *7*, 15894−15902.

(19) Qi, X.; Chang, C.; Xu, X.; Zhang, Y.; Bai, Y.; Liu, H. Magnetization of 3-dimentional homochiral metal-organic frameworks for efficient and highly selective capture of phosphopeptides. *J. Chromatogr. A* **2016**, *1468*, 49−54.

(20) Zhao, M.; Zhang, X.; Deng, C. Facile synthesis of hydrophilic magnetic graphene@metal-organic framework for highly selective enrichment of phosphopeptides. *RSC Adv.* **2015**, *5*, 35361−35364.

(21) Xie, Y.; Deng, C. Highly efficient enrichment of phosphopeptides by a magnetic lanthanide metal-organic framework. *Talanta* **2016**, *159*, 1−6.

(22) Chen, Y.; Xiong, Z.; Peng, L.; Gan, Y.; Zhao, Y.; Shen, J.; Qian, J.; Zhang, L.; Zhang, W. Facile preparation of core-shell magnetic metal organic framework nanoparticles for the selective capture of phosphopeptides. *ACS Appl. Mater. Interfaces* **2015**, *7*, 16338−16347.

(23) Huan, W.; Xing, M.; Cheng, C.; Li, J. Facile fabrication of magnetic metal-organic framework nanofibers for specific capture of phosphorylated peptides. *ACS Sustainable Chem. Eng.* **2019**, *7*, 2245−2254.
(24) Xie, Y.; Deng, C. Designed synthesis of a "one for two" hydrophilic magnetic amino-functionalized metal-organic framework for highly efficient enrichment of glycopeptides and phosphopeptides. *Sci. Rep.* **2017**, *7*, 1162.
(25) Wu, Y.; Liu, Q.; Xie, Y.; Deng, C. Core-shell structured magnetic metal-organic framework composites for highly selective enrichment of endogenous N-linked glycopeptides and phosphopeptides. *Talanta* **2018**, *190*, 298−312.
(26) Wu, Y.; Liu, Q.; Deng, C. L-cysteine-modified metal-organic frameworks as multifunctional probes for efficient identification of N-linked glycopeptides and phosphopeptides in human crystalline lens. *Anal. Chim. Acta* **2019**, *1061*, 110−121.
(27) Liu, B.; Lu, Y.; Wang, B.; Yan, Y.; Liang, H.; Yang, H. Facile preparation of hydrophilic dual functional magnetic metal-organic frameworks as a platform for proteomics research. *ChemistrySelect* **2019**, *4*, 2200−2204.
(28) Luo, B.; Chen, Q.; He, J.; Li, Z.; Yu, L.; Lan, F.; Wu, Y. Boronic acid-functionalized magnetic metal-organic frameworks via a dual-ligand strategy for highly efficient enrichment of phosphopeptides and glycopeptides. *ACS Sustainable Chem. Eng.* **2019**, *7*, 6043−6052.
(29) Liu, Q.; Sun, N.; Gao, M.; Deng, C.-h. Magnetic binary metal-organic framework as a novel affinity probe for highly selective capture of endogenous phosphopeptides. *ACS Sustainable Chem. Eng.* **2018**, *6*, 4382−4389.
(30) Xiao, R.; Pan, Y.; Li, J.; Zhang, L.; Zhang, W. Layer-by-layer assembled magnetic bimetallic metal-organic framework composite for global phosphopeptide enrichment. *J. Chromatogr. A* **2019**, *1601*, 45−52.
(31) Yuan, S.; Chen, Y.-P.; Qin, J.; Lu, W.; Wang, X.; Zhang, Q.; Bosch, M.; Liu, T.-F.; Lian, X.; Zhou, H.-C. Cooperative cluster metalation and ligand migration in zirconium metal-organic frameworks. *Angew. Chem., Int. Ed.* **2015**, *127*, 14909−14913.
(32) Deng, H.; Li, X.; Peng, Q.; Wang, X.; Chen, J.; Li, Y. Monodisperse magnetic single-crystal ferrite microspheres. *Angew. Chem., Int. Ed.* **2005**, *117*, 2842−2845.
(33) Long, X.-y.; Song, Q.; Lian, H.-z. Development of magnetic LuPO4 microspheres for highly selective enrichment and identification of phosphopeptides for MALDI-TOF MS analysis. *J. Mater. Chem. B* **2015**, *3*, 9330−9339.
(34) Long, X.-Y.; Li, J.-Y.; Sheng, D.; Lian, H.-Z. Spinel-type manganese ferrite ($MnFe_2O_4$) microspheres: A novel affinity probe for selective and fast enrichment of phosphopeptides. *Talanta* **2017**, *166*, 36−45.
(35) Li, J.-y.; Long, X.-y.; Sheng, D.; Lian, H.-z. Organic molecule-assisted synthesis of Fe_3O_4/graphene oxides nanocomposite for selective capture of low-abundance peptides and phosphopeptides. *Talanta* **2020**, *208*, 120437.
(36) Li, J.-y.; Cao, Z.-m.; Hua, Y.; Wei, G.; Yu, X.-z.; Shang, W.-b.; Lian, H.-z. Solvothermal synthesis of novel magnetic nickel based iron oxide nanocomposites for selective capture of global- and mono-phosphopeptides. *Anal. Chem.* **2020**, *92*, 1058−1067.
(37) Boersema, P. J.; Raijmakers, R.; Lemeer, S.; Mohammed, S.; Heck, A. J. R. Multiplex peptide stable isotope dimethyl labeling for quantitative proteomics. *Nat. Protoc.* **2009**, *4*, 484−494.
(38) Shpitzer, T.; Hamzany, Y.; Bahar, G.; Feinmesser, R.; Savulescu, D.; Borovoi, I.; Gavish, M.; Nagler, R. M. Salivary analysis of oral cancer biomarkers. *Br. J. Cancer* **2009**, *101*, 1194−1198.
(39) Long, X.-y.; Li, J.-y.; Sheng, D.; Lian, H.-z. Low-cost iron oxide magnetic nanoclusters affinity probe for the enrichment of endogenous phosphopeptides in human saliva. *RSC Adv.* **2016**, *6*, 96210−96222.

https://dx.doi.org/10.1021/acssuschemeng.0c04118
ACS Sustainable Chem. Eng. 2020, 8, 16422−16429